DALTON
FULL PAPER

Hydrothermal synthesis, crystal structure and thermal transformation of a new zinc arsenate hydrate, $Zn_9(AsO_4)_6{\cdot}4H_2O$ †

Torben R. Jensen,*[a] Poul Norby,[b] Jonathan C. Hanson,[c] Eivind M. Skou[a] and P. C. Stein[a]

[a] *Chemistry Department, University of Odense, DK-5230 Odense M, Denmark*
[b] *Department of Chemistry, State University of New York at Stony Brook, Stony Brook, NY 11794, USA*
[c] *Chemistry Department, Brookhaven National Laboratory, Upton 11973, NY, USA*

A new synthetic polymorph of zinc arsenate hydrate, $Zn_9(AsO_4)_6{\cdot}4H_2O$, was prepared from an aqueous solution. Owing to the small size of the crystals, synchrotron X-ray radiation was applied for the indexing and data collection. An initial structural model was found from 1819 unique reflections measured (space group $P\bar{1}$, refined to $wR = 0.154$, $R = 0.060$). Optimisation of the synthesis conditions provided larger crystals for crystallographic measurements using a conventional diffractometer: $a = 6.6895(3)$, $b = 9.1761(4)$, $c = 10.1377(8)$ Å, $\alpha = 69.428(5)$, $\beta = 77.205(5)$, $\gamma = 75.765(4)°$, space group $P\bar{1}$. The structure was refined to $wR = 0.072$, $R = 0.061$. The crystal structure of $Zn_9(AsO_4)_6{\cdot}4H_2O$ is built from chains of edge-sharing octahedra and trigonal-bipyramidal Zn atoms co-ordinated to framework oxygen and water molecule oxygen atoms. These chains are connected by tetrahedra of Zn and As co-ordinated to framework oxygen atoms. Channels run along the *a* axis where the water molecules are placed. The compound transforms into a new phase of $Zn_3(AsO_4)_2$ at 424(1) °C and into the known phase β-$Zn_3(AsO_4)_2$ at 865(1) °C.

Several compounds in the systems, $ZnO–As_2O_5–H_2O$ and $ZnO–P_2O_5–H_2O$ are found in nature as minerals, while synthetic members are sparse. Zinc orthoarsenates and orthophosphates have a rich crystal chemistry mainly due to the co-ordination flexibility of the zinc ions, which can form polyhedra by co-ordinating to four, five or six oxygen atoms. This gives a large span in the extent of hydration found in these materials. The zinc polyhedra can be assembled in chains by face, edge or vertice sharing. These chains are connected with discrete arsenate or phosphate tetrahedra by vertex sharing. Generally the co-ordination number of zinc decreases with decreasing number of water molecules in the crystal structure. The most hydrated compounds belong to the vivianite group of minerals, $M_3(TO_4)_2{\cdot}8H_2O$, with T = As or P. In the orthoarsenates, M = Mg, Fe, Co, Ni or Zn and in the related orthophosphates M = Fe or Mg.[1] Two polymorphs exist of the most hydrated zinc orthophosphate, $Zn_3(PO_4)_2{\cdot}4H_2O$ hopeite and parahopeite both containing zinc octahedra and tetrahedra.[2] Thermogravimetric measurements of hopeite indicated the existence of three other polymorphs, $Zn_3(PO_4)_2{\cdot}xH_2O$, $x = 3$, 2.5 or 2. The detailed structures are unknown, but a monoclinic unit cell related to hopeite was suggested for the dihydrate.[3] A synthetic zinc phosphate monohydrate, $Zn_3(PO_4)_2{\cdot}H_2O$, was described containing four- and five-co-ordinated zinc ions.[4]

The product upon complete dehydration of the mentioned zinc orthophosphates is α-$Zn_3(PO_4)_2$. At 942 °C α-$Zn_3(PO_4)_2$ transforms to β-$Zn_3(PO_4)_2$ which can be quenched to room temperature. Another polymorph, γ-$Zn_3(PO_4)_2$, was stabilised using a small amount of manganese ions. In the crystal structure of α-$Zn_3(PO_4)_2$ zinc is co-ordinated to four oxygen atoms, in β-$Zn_3(PO_4)_2$ to four and five and in γ-$Zn_3(PO_4)_2$, to four and six.[5]

The zinc orthoarsenates are less investigated. The mineral köttigite, $Zn_3(AsO_4)_2{\cdot}8H_2O$, is built from edge-sharing zinc octahedra connected by discrete arsenate tetrahedra.[1a] Comparison of unit-cell parameters indicated that the synthetic zinc arsenate, $Zn_3(AsO_4)_2{\cdot}4H_2O$, is isomorphous with parahopeite.[6] The mineral warikahnit, $Zn_3(AsO_4)_2{\cdot}2H_2O$, was found to contain zinc tetrahedra, trigonal bipyramids and octahedra forming a complex structure.[7] Prosperite, $Ca_2Zn_4(AsO_4)_4{\cdot}H_2O$, an orthoarsenate mineral with the lowest number of crystal water molecules, was described as having a complex structure built from five-co-ordinated zinc atoms.[8] Zinc orthoarsenates with no crystal water are known in two modifications, α- and β-$Zn_3(AsO_4)_2$. The former was found to be isomorphous with β-$Zn_3(PO_4)_2$ and β-$Zn_3(AsO_4)_2$ is isomorphous with γ-$Zn_3(PO_4)_2$,[9] demonstrating the similarities in the crystal chemistry in the orthoarsenates and orthophosphates. Several hydrogen and hydroxide orthoarsenates and orthophosphates are known to show similarities in the crystal chemistry as well, *e.g.* the adamite-like materials $M_2(TO_4)(OH)$, with T = As or P and M = Zn or Co.[10]

The phase $Zn_9(AsO_4)_6{\cdot}4H_2O$ presented in this study is the second example of a synthetic zinc orthoarsenate hydrate which is not known as a mineral.[11] We report the synthesis and refined structural parameters of this new zinc arsenate hydrate. Two crystal morphologies were found and studied by two different single-crystal diffraction techniques. The refined structural models were identical and are reported along with powder diffraction data and a thermal investigation using thermogravimetry (TG) and differential scanning calorimetry (DSC).

Experimental

Hydrothermal synthesis

The system $H_3AsO_4–Zn(NO_3)_2–LiOH–H_2O$ was investigated using different amounts of LiOH and different temperatures, in order to evaluate the formation regions of lithium zinc arsenates and zinc arsenate hydrates. Synthesis **I** was performed as described elsewhere,[12] using a molar ratio of the reactants $H_3AsO_4 : Zn(NO_3)_2 : LiOH : H_2O = 1.0 : 1.0 : 2.8 : \approx 175$ and $[AsO_4^{3-}] = 0.30$ M, pH 2.5. This mixture was placed at a constant temperature of 240 °C for 43 h and the resulting yield was 0.639 g crystalline material, batch **I**. In order to prepare $Zn_9(AsO_4)_6{\cdot}4H_2O$ for further characterisation the following synthesis, **II**, was performed. A clear solution of H_3AsO_4 (3.731 g) and $Zn(NO_3)_2{\cdot}6H_2O$ (11.958 g) dissolved in water (40 cm^3) was prepared and added, with stirring, to a solution of $LiOH{\cdot}H_2O$ (1.994 g) dissolved in water (100 cm^3) in a Teflon-lined steel autoclave. The molar ratio of the reactants was H_3AsO_4:

† *Non-SI unit employed*: eV ≈ 1.60×10^{-19} J.

$Zn(NO_3)_2 : LiOH : H_2O = 1.0 : 1.9 : 2.3 : \approx 380$, and $[AsO_4^{3-}] = 0.15$ M. This gel slurry was heated at a constant temperature of 240 °C for 47 h. Upon cooling and recovery of the crystalline material, batch **II**, by vacuum filtration and washing with water, the yield of crystals (up to 2.5 mm in size) was 3.678 g. The pH of the crystallising fluid was 1.6.

The synthesis was performed using the following chemicals: $LiOH \cdot H_2O$ (Fluka, puriss p.a. >99%), H_3AsO_4 (Merck, extra pure, 80%) and $Zn(NO_3)_2 \cdot 6H_2O$ (Fluka Chemie AG, purum p.a. >99.0%). The precise water content in lithium hydroxide monohydrate was determined by thermogravimetry to be $LiOH \cdot 1.00H_2O$. **CAUTION**: arsenic acid is highly toxic and extremely liable to cause dermatitis.

Powder diffraction

Powder diffraction data for determining and refining unit-cell parameters were obtained using a Siemens D5000 diffractometer equipped with a primary germanium monochromator (Cu-Kα_1 radiation, $\lambda = 1.540\,598$ Å). The samples were mounted on a flat glass plate. The data were collected from 5 to 90° in 2θ with a step length of 0.02° and a counting time of 15 s per step. The program CELLKANT[13] was used to refine the unit-cell parameters from the observed *d* spacings. The program POWDER CELL[14] was used for calculation of the powder patterns of α- and β-$Zn_3(AsO_4)_2$ for identification of the thermal decomposition products. Powder patterns were simulated using unit-cell parameters, atomic positions and the space groups found in ref. 9.

Solid-state NMR spectroscopy

Magic angle spinning ^{7}Li NMR spectra were recorded on a Varian UNITY-500 spectrometer [11.7 T, $\nu(^7Li) = 194.3$ MHz], using a Jakobsen MAS probe,[15] as described elsewhere.[12]

Thermal investigation

A phase-pure sample of $Zn_9(AsO_4)_6 \cdot 4H_2O$, obtained by hand-sorting sample **II**, was used for the thermal investigation. Thermogravimetric measurements were performed between room temperatures and 600 °C, using a SETARAM TG 92-12 instrument, a nitrogen atmosphere and heating rate of 5 °C min^{-1}. The sample was kept in an open Al_2O_3 crucible. Differential scanning calorimetry was performed using a SETARAM DTA 92-16.18 instrument. The sample was placed in a platinum crucible and α-Al_2O_3 used as a reference. The experiment was carried out in an argon atmosphere between 20 and 900 °C using a heating rate of 5 °C min^{-1} and a cooling rate of 10 °C min^{-1}. For investigation of eventual reversible phase transitions this heating and cooling procedure was repeated using the same sample. The temperature and enthalpy change calibrations were carried out using the low–high quartz transition and the dehydration of $CaSO_4 \cdot 2H_2O$ as standards.

Phase identification

Optical microscopy of batch **I** revealed crystals with three distinct morphologies, hexagonal rods, plate-like crystals (<30% w/w) and octahedra-like crystals (<5% w/w). Indexing of triclinic materials using powder diffraction data can give ambiguous results, especially when other phases are present in the sample, as in this case. Single-crystal diffraction using an image plate (IP) area detector combined with the intense synchrotron X-ray radiation can give a fast and reliable estimate of the unit-cell parameters of microcrystals with dimensions of tens of μm. Data were collected at the synchrotron radiation facility at beamline X7B, NSLS, Brookhaven National Laboratory,[16] for indexing of two of the phases found in sample **I**.

A plate-like crystal of $Zn_9(AsO_4)_6 \cdot 4H_2O$ was found to have a triclinic unit cell ($a = 6.66$, $b = 9.15$, $c = 10.10$ Å, $\alpha = 69.77$, $\beta = 77.59$, $\gamma = 76.00$°) and an octahedra-like crystal was orthorhombic ($a = 8.38$, $b = 8.42$, $c = 6.05$ Å). The latter material appeared to be the known adamite phase, $Zn_2(AsO_4)(OH)$.[10a] Diffraction data from two independent IPs gave similar results, with the same unit-cell volume but minor differences in the axes. The main component of batch **I**, hexagonal rods, was identified as α-$LiZnAsO_4$ [$a_h = 14.0417(6)$, $c_h = 9.3801(8)$ Å] using powder diffraction data. A micro single crystal of α-$LiZnAsO_4$ (17 × 17 × 60 μm) was selected from this batch and used for the data collection and refinement of the phenacite-type structure (space group *R*3).[12]

Batch **II** contained crystals of three morphologies that could be sorted by hand, plate-like crystals (≈85% w/w) and octahedra-like crystals (≈14% w/w) along with a small fraction of thin needle-like crystals (<2% w/w). The latter is possibly α-$LiZnAsO_4$. The octahedra-like crystals were identified as adamite, $Zn_2(AsO_4)(OH)$,[10a] using powder diffraction [refined unit-cell parameters: $a = 8.3191(9)$, $b = 8.523(1)$, $c = 6.054(1)$ Å]. A fragment of a plate-like crystal was indexed using 25 reflections measured by an Enraf-Nonius CAD-4F diffractometer ($\lambda = 1.541\,78$ Å). A triclinic unit cell was found: $a = 6.6895(3)$, $b = 9.1761(4)$, $c = 10.1377(8)$ Å, $\alpha = 69.428(5)$, $\beta = 77.205(5)$, $\gamma = 75.765(4)$°.

The morphologies of the plate-like crystals from syntheses **I** and **II** were different. Synthesis **I** gave independent single crystals with visible angles between the faces. The crystals from synthesis **II** were propeller like, *i.e.* two elongated plates growing from a common centre with no pronounced angles between faces.

Structure determination and refinement

Synchrotron X-ray diffraction. A clear, colourless plate-like single crystal of $Zn_9(AsO_4)_6 \cdot 4H_2O$ was selected from batch **I**. Owing to its small size synchrotron X-ray radiation ($\lambda = 0.9540$ Å) and an image plate (Fuji Type V, 200 × 250 mm) as area detector were used for the data collections as previously described.[12] The experimental details are given in Table 1. The 44 image plates in the data set were scaled together by comparing symmetry-related reflections yielding 1819 unique observations. The scale factors provide a correction of the data for the intensity decay of the synchrotron radiation. A Lorentz-polarisation correction was applied, using the program DENZO.[17] Absorption was neglected due to the small size of the crystal. The wavelength used, $\lambda = 0.9540$ Å (13.0 keV), was below the K-edge of arsenic ($\lambda = 1.044$ Å, 11.865 keV) and zinc ($\lambda = 1.283$ Å, 9.6607 keV).[18] The program FPRIME in the GSAS structure refinement program(s)[19] was used to estimate f' and f'' giving values of −1.493 and 3.225 for arsenic and −0.219 and 2.372 for zinc, respectively.

A structural model was found using direct methods in space group $P\bar{1}$, no. 2. The oxygen atoms were refined with isotropic thermal parameters and the cations anisotropically. The refinement converged on $wR = 0.154$ and $R = 0.060$, with 127 parameters refined, using full-matrix least squares based on F^2 and a weighting scheme $w = [\sigma^2(F_o^2) + 0.109P^2]^{-1}$, where $P = (F_o^2 + 2F_c^2)/3$. The program Siemens SHELXTL™, version 5.0[20] was used for structure solution and refinement.

Conventional X-ray diffraction. The crystal size of $Zn_9(AsO_4)_6 \cdot 4H_2O$ found in batch **II** allowed single-crystal data collection using a conventional technique with graphite-monochromatised Cu-Kα radiation, $\lambda = 1.541\,78$ Å. The experimental details are given in Table 1. A standard reflection measured every 100 min showed no significant intensity change. Data were corrected for Lorentz-polarisation effects and for absorption giving 2211 unique reflections. The absorption correction was performed using Gaussian integration. Programs from the XTAL 3.2[21] system were used to solve and refine the

Table 1 Crystal data and details of data collection and structure refinement for $Zn_9(AsO_4)_6{\cdot}4H_2O$

	Odense	Beamline X7B, Brookhaven
a/Å	6.6895(3)	6.66
b/Å	9.1761(4)	9.15
c/Å	10.1377(8)	10.10
α/°	69.428(5)	69.77
β/°	77.205(5)	77.59
γ/°	75.765(4)	76.00
U/Å^3	558.43(6)	—
D_c/g cm^{-3}	4.443	—
Crystal size/mm	0.33 × 0.10 × 0.07	0.083 × 0.066 × 0.012
No. of reflections for cell parameters	25	37
Diffractometer	Enraf-Nonius CAD-4F	Huber
λ/Å	1.54178	0.9540
X-Ray generator	Cu-Kα Sealed tube	Storage ring
Scan method	ω–2θ	ω
Scan range, θ_{min}, θ_{max}/°	4.71, 73.86	2.92, 44.37
μ/mm^{-1}	21.64	—
F(000)	700	692.0
T_{min}, T_{max}	0.122, 0.362	—
Range of h, k, l	−8 to 7, −10 to 11, 0–12	−8 to 7, −12 to 13, 0–12
Total data	2211	1819
Observed data	2201 [$I > 2\sigma(I)$]	1507 [$F_o^2 > 2\sigma(F_o^2)$]
Refinement, full matrix on	F	F^2
Reflections used	2201	1809
Parameters	197	127
R_{obs}, R_{all}	0.061, 0.061	0.0596, 0.0730
wR_{obs}, wR_{all}	0.072, 0.072	0.1540, 0.2229
$\Delta\rho_{min}$, $\Delta\rho_{max}$/e Å^{-3}	−2.39, 3.70	−1.80, 2.14

Common parameters: data collection temperature, 23(2) °C, on colourless cut plate-like crystals; $As_6O_{24}Zn_9{\cdot}4H_2O$, M 1494.00; triclinic, space group $P\bar{1}$; $Z = 1$.

crystal structure, using full-matrix least-squares methods on F and anisotropic thermal parameters. The refinement converged on $wR = 0.072$ and $R = 0.061$, with 197 parameters refined, using a weighting scheme $w = 1/\sigma(F_o)$. The holes and peaks in the Fourier map were close to the positions of the heavy atoms. It was not possible to locate the positions of the hydrogen atoms. Scattering factors of neutral atoms were applied throughout this work.

CCDC reference number 186/820.

Results and Discussion

Lithium-7 MAS NMR spectroscopy on sample **II** showed only one faint signal with chemical shift δ 0.2, which is due to a small amount of α-$LiZnAsO_4$ present.[12] This supports the crystallographic data which show no presence of Li in $Zn_9(AsO_4)_6{\cdot}4H_2O$. Thermogravimetric measurements were in accordance with the formula $Zn_9(AsO_4)_6{\cdot}4H_2O$, observed weight loss 4.60% at 349–410 °C (calculated 4.82%). Fig. 2 shows that the dehydration is a one-step reaction.

Crystal structure

The structural models found from the two data sets obtained under different experimental conditions on crystals of $Zn_9(AsO_4)_6{\cdot}4H_2O$ from two different samples were identical. The data obtained using the conventional single-crystal diffraction technique will be discussed in the following. The crystal structure refinement revealed an orthoarsenate with three unique arsenic tetrahedra. There are five unique zinc positions, three of which are octahedrally co-ordinated to oxygen, one trigonal

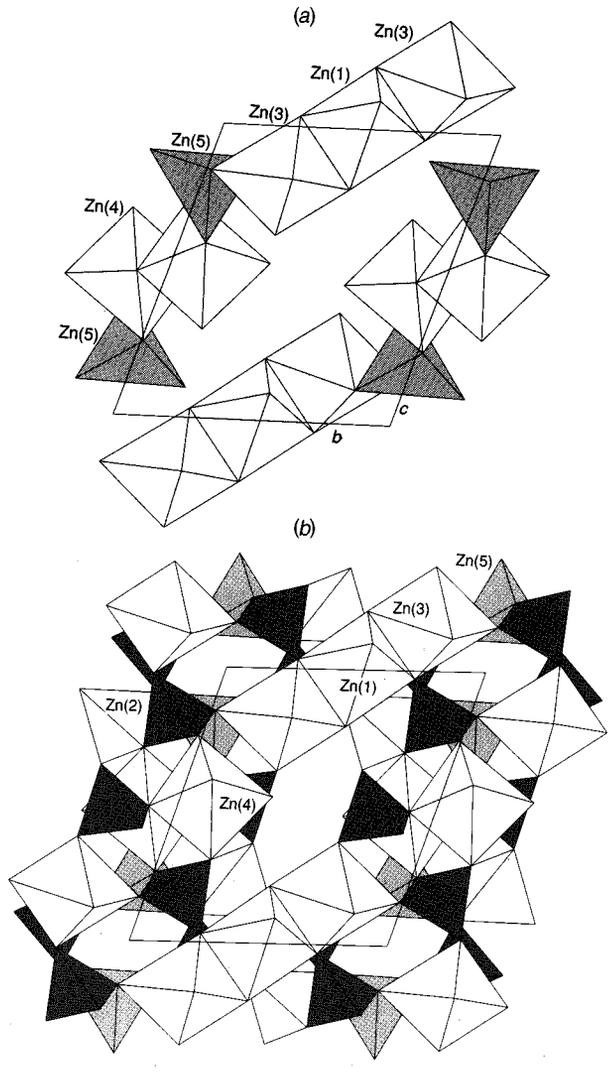

Fig. 1 Crystal structure of $Zn_9(AsO_4)_6{\cdot}4H_2O$ viewed along the a axis: (*a*) illustrates chains of edge-sharing zinc polyhedra; (*b*) shows channels parallel to the a axis containing water molecules. Zinc octahedra and tetrahedra are unshaded, zinc trigonal bipyramids are grey and arsenic tetrahedra are black

bipyramidal and one with tetrahedral co-ordination to oxygen. The Zn(1) octahedron has centrosymmetry because Zn(1) is placed on the special position $(0,0,\frac{1}{2})$; the Zn(3) and Zn(4) octahedra are more irregular. The Zn(1) octahedron is co-ordinated to two water oxygen atoms, Zn(3) and Zn(4) to one. The Zn(2) tetrahedron is slightly more irregular than the arsenic tetrahedra. The trigonal bipyramid of Zn(5) is slightly irregular with O(2), O(4) and O(5) almost lying in a plane and an elongated bond Zn(5)–O(12). Atom Zn(1) surrounded by two Zn(3) participates in segments of three octahedra connected by Zn(4) octahedra and Zn(5) trigonal bipyramids. The edge-sharing zinc polyhedra form infinite zigzag chains, approximately in the (111) direction, as illustrated on Fig. 1(*a*). The distinct chains are connected by arsenic and Zn(2) tetrahedra. The resulting structure of $Zn_9(AsO_4)_6{\cdot}4H_2O$ is displayed in Fig. 1(*b*). Channels in the crystal structure, along the a axis, contain water molecules.

Selected bond lengths and angles are given in Table 2. Oxidation states, V_i, were calculated as a sum of bond valences, s, using the equation $s = \exp[(r_o - r)/B]$, where r_o and B are empirical parameters [r_o(As–O) = 1.767, r_o(Zn–O) = 1.704, and $B = 0.37$] and r is the refined bond length.[22] The values of the cations, given in Table 3, are in agreement with the expected oxidation states. Framework oxygen atoms co-ordinated to three cations have calculated oxidation states in the range

Table 2 Selected bond lengths (Å) and angles (°). Symmetry transformations used to generate equivalent atoms: (*i*) $+x$, $+y$, $+z+1$, (*ii*) $-x$, $-y+1$, $-z+1$, (*iii*) $-x+1$, $-y+1$, $-z+1$, (*iv*) $+x$, $+y+1$, $+z$, (*v*) $+x-1$, $+y+1$, $+z$, (*vi*) $+x+1$, $+y$, $+z+1$, (*vii*) $+x$, $+y+1$, $+z+1$, (*viii*) $-x+1$, $-y$, $-z+2$

As(1^{i})–O(2^{i})	1.696(9)	Zn(3)–O(1^{iii})	2.04(1)
As(1^{i})–O(3^{i})	1.692(8)	Zn(3)–O(5^{iv})	2.39(1)
As(1^{i})–O(6^{i})	1.67(1)	Zn(3)–O(13^{ii})	2.47(1)
As(1^{i})–O(7^{i})	1.68(1)	Zn(3)–O(11^{v})	2.034(9)
		Zn(3)–O(6)	2.000(8)
As(2^{ii})–O(1^{iii})	1.710(7)	Zn(3)–O(12)	2.023(9)
As(2^{ii})–O(9^{ii})	1.711(9)		
As(2^{ii})–O(12^{ii})	1.67(1)	Zn(4^{i})–O(2^{i})	2.08(1)
As(2^{ii})–O(10^{iii})	1.668(9)	Zn(4^{i})–O(9^{iii})	2.123(9)
		Zn(4^{i})–O(10^{i})	2.176(8)
As(3^{iv})–O(4^{iv})	1.701(9)	Zn(4^{i})–O(14^{i})	2.13(1)
As(3^{iv})–O(5^{iv})	1.66(1)	Zn(4^{i})–O(7^{vi})	2.08(1)
As(3^{iv})–O(8^{iv})	1.706(8)	Zn(4^{i})–O(7^{iii})	2.11(1)
As(3^{iv})–O(11^{iv})	1.673(9)		
		Zn(5^{i})–O(2^{i})	2.001(9)
Zn(1^{v})–O(1^{iii})	2 × 2.058(9)	Zn(5^{i})–O(10^{i})	2.05(1)
Zn(1^{v})–O(8^{iv})	2 × 2.210(9)	Zn(5^{i})–O(12^{i})	2.25(1)
Zn(1^{v})–O(13^{ii})	2 × 2.07(1)	Zn(5^{i})–O(5^{vii})	1.93(1)
		Zn(5^{i})–O(4^{viii})	1.978(8)
Zn(2^{iii})–O(3^{i})	1.875(9)		
Zn(2^{iii})–O(4^{iv})	1.97(1)		
Zn(2^{iii})–O(9^{iii})	1.971(9)		
Zn(2^{iii})–O(8^{iii})	1.940(8)		
O(2^{i})–As(1)–O(3^{i})	108.6(4)	O(1^{iii})–Zn(3)–O(5^{iv})	75.1(4)
O(2^{i})–As(1^{i})–O(6^{i})	111.0(5)	O(1^{iii})–Zn(3)–O(13^{ii})	76.9(3)
O(2^{i})–As(1^{i})–O(7^{i})	108.7(5)	O(1^{iii})–Zn(3)–O(11^{v})	95.5(4)
O(3^{i})–As(1^{i})–O(6^{i})	106.0(4)	O(1^{iii})–Zn(3)–O(6)	146.3(4)
O(3^{i})–As(1^{i})–O(7^{i})	108.7(5)	O(1^{iii})–Zn(3)–O(12)	109.5(3)
O(6^{i})–As(1^{i})–O(7^{i})	113.6(5)	O(5^{iv})–Zn(3)–O(13^{ii})	100.3(4)
		O(5^{iv})–Zn(3)–O(11^{v})	170.5(4)
O(1^{iii})–As(2^{ii})–O(9^{ii})	101.2(4)	O(5^{iv})–Zn(3)–O(6)	89.5(4)
O(1^{iii})–As(2^{ii})–O(12^{ii})	109.8(5)	O(5^{iv})–Zn(3)–O(12)	74.0(4)
O(1^{iii})–As(2^{ii})–O(10^{iii})	114.7(4)	O(13^{ii})–Zn(3)–O(11^{v})	75.7(4)
O(9^{ii})–As(2^{ii})–O(12^{ii})	110.8(5)	O(13^{ii})–Zn(3)–O(6)	76.7(4)
O(9^{ii})–As(2^{ii})–O(10^{iii})	111.0(5)	O(13^{ii})–Zn(3)–O(12)	169.5(3)
O(12^{ii})–As(2^{ii})–O(10^{iii})	109.1(5)	O(11^{v})–Zn(3)–O(6)	97.9(4)
		O(11^{v})–Zn(3)–O(12)	111.2(4)
O(4^{iv})–As(3^{iv})–O(5^{iv})	108.1(5)	O(6)–Zn(3)–O(12)	94.2(4)
O(4^{iv})–As(3^{iv})–O(8^{iv})	103.8(4)		
O(4^{iv})–As(3^{iv})–O(11^{iv})	113.7(5)	O(2^{i})–Zn(4^{i})–O(9^{iii})	103.1(4)
O(5^{iv})–As(3^{iv})–O(8^{iv})	109.1(5)	O(2^{i})–Zn(4^{i})–O(10^{i})	78.8(4)
O(5^{iv})–As(3^{iv})–O(11^{iv})	111.6(5)	O(2^{i})–Zn(4)–O(14^{i})	89.2(4)
O(8^{iv})–As(3^{iv})–O(11^{iv})	110.3(4)	O(2^{i})–Zn(4)–O(7^{vi})	165.4(3)
		O(2^{i})–Zn(4)–O(7^{iii})	94.6(4)
O(1^{iii})–Zn(1^{v})–O(8^{iv})	89.9(3)	O(9^{iii})–Zn(4)–O(10^{i})	169.6(4)
O(1^{iii})–Zn(1^{v})–O(13^{ii})	86.3(4)	O(9^{iii})–Zn(4)–O(14^{i})	90.2(4)
O(1^{iii})–Zn(1^{v})–O(1^{v})	180.0(5)	O(9^{iii})–Zn(4)–O(7^{vi})	91.4(4)
O(1^{iii})–Zn(1^{v})–O(8^{ii})	90.1(3)	O(9^{iii})–Zn(4)–O(7^{iii})	82.6(3)
O(1^{iii})–Zn(1^{v})–O(13^{iv})	93.7(4)	O(10^{i})–Zn(4)–O(14^{i})	100.1(4)
O(8^{iv})–Zn(1^{v})–O(13^{ii})	80.2(4)	O(10^{i})–Zn(4)–O(7^{vi})	86.6(4)
O(8^{iv})–Zn(1^{v})–O(1^{v})	90.1(3)	O(10^{i})–Zn(4)–O(7^{iii})	87.0(3)
O(8^{iv})–Zn(1^{v})–O(8^{ii})	180.0(6)	O(14^{i})–Zn(4)–O(7^{vi})	92.8(4)
O(8^{iv})–Zn(1^{v})–O(13^{iv})	99.8(4)	O(14^{i})–Zn(4)–O(7^{iii})	172.4(3)
O(13^{ii})–Zn(1^{v})–O(1^{v})	93.7(4)	O(7^{vi})–Zn(4)–O(7^{iii})	85.2(4)
O(13^{ii})–Zn(1^{v})–O(8^{ii})	99.8(4)		
O(13^{ii})–Zn(1^{v})–O(13^{iv})	180.0(3)	O(2^{i})–Zn(5^{i})–O(10^{i})	83.7(4)
O(1^{v})–Zn(1^{v})–O(8^{ii})	89.9(3)	O(2^{i})–Zn(5^{i})–O(12^{i})	91.8(4)
O(1^{v})–Zn(1^{v})–O(13^{iv})	86.3(4)	O(2^{i})–Zn(5^{i})–O(5^{vii})	108.4(4)
O(8^{ii})–Zn(1^{v})–O(13^{iv})	80.2(4)	O(2^{i})–Zn(5^{i})–O(4^{viii})	121.2(4)
		O(10^{i})–Zn(5^{i})–O(12^{i})	173.9(4)
O(3^{i})–Zn(2^{iii})–O(4^{iv})	108.1(5)		
O(3^{i})–Zn(2^{iii})–O(9^{iii})	111.1(4)	O(10^{i})–Zn(5^{i})–O(5^{vii})	106.3(4)
O(3^{i})–Zn(2^{iii})–O(8^{iii})	121.8(4)	O(10^{i})–Zn(5^{i})–O(4^{viii})	95.3(4)
O(4^{iv})–Zn(2^{iii})–O(9^{iii})	103.5(4)	O(12^{i})–Zn(5^{i})–O(5^{vii})	79.0(4)
O(4^{iv})–Zn(2^{iii})–O(8^{iii})	108.5(4)	O(12^{i})–Zn(5^{i})–O(4^{viii})	83.5(4)
O(9^{iii})–Zn(2^{iii})–O(8^{iii})	102.2(4)	O(5^{vii})–Zn(5^{i})–O(4^{viii})	127.6(4)

1.94 to 2.17. The framework oxygen atoms co-ordinated to two cations have lower V_i, 1.70 to 1.86, possibly due to a bond-valence contribution from hydrogen bonding. When the bond-valence contributions from the hydrogen atoms were not included significantly lower V_i, 0.50 and 0.32, were obtained for the oxygen atoms in the water molecules, O(13) and O(14).

Thermal investigation

Differential scanning calorimetry revealed two endothermic events upon heating $Zn_9(AsO_4)_6{\cdot}4H_2O$ to 900 °C, as illustrated in Fig. 2. There was no thermal event on the cooling curve or in the following experiment using the same sample, showing the structural changes to be irreversible. One enthalpy change was

Table 3 Calculated oxidation states, V_i, for the ions in the structure of $Zn_9(AsO_4)_6{\cdot}4H_2O$, using ref. 22

Cation	No.	V_i	Co-ordination number
Arsenic	1	5.02	4
	2	4.95	4
	3	5.00	4
Zinc	1	2.02	6
	2	2.14	4
	3	1.97	6
	4	1.97	6
	5	2.09	5
Oxygen	No.	V_i	Co-ordination number
Framework	1	1.94	3
	2	2.02	3
	3	1.86	2
	4	2.17	3
	5	2.03	3
	6	1.76	2
	7	1.96	3
	8	1.96	3
	9	1.97	3
	10	1.98	3
	11	1.70	2
	12	1.96	3
Water	13	0.50	2
	14	0.32	1

Table 4 Observed reflections (*d* spacing and intensity) of a new polymorph of $Zn_3(AsO_4)_2$ prepared by heating $Zn_9(AsO_4)_6{\cdot}4H_2O$ to 500 °C

d/Å	I/I_o	*d*/Å	I/I_o	*d*/Å	I/I_o
5.3820	9	3.0178	14	2.3157	12
4.8657	9	2.9467	12	2.3001	13
4.7341	13	2.8746	45	2.2404	16
4.4571	9	2.8245	18	2.1908	6
4.2252	23	2.7319	50	2.1153	12
4.0900	9	2.6187	8	2.0738	9
3.9972	11	2.5680	38	2.0437	10
3.9037	8	2.5062	9	1.9066	8
3.6679	17	2.4691	20	1.8408	10
3.5842	22	2.4432	17	1.8164	10
3.2212	31	2.3669	10	1.7283	9
3.1645	100	2.3492	8	1.6947	14
3.0813	28				

associated with a weight loss detected by TG, which is due to dehydration as illustrated in Fig. 2. The enthalpy change was determined by $\Delta H = 116(24)$ J g^{-1}, with peak value at 424(1) °C. The second endothermic event was weaker, giving $\Delta H = 8(2)$ J g^{-1}, with a peak value of 865(1) °C.

The product after the two DSC experiments (heating to 900 °C) was identified as β-$Zn_3(AsO_4)_2$ using powder diffraction and a calculated powder pattern. The refined unit-cell parameters are in agreement with those of β-$Zn_3(AsO_4)_2$ (ref. 9), $a = 5.278(2)$, $b = 8.495(3)$, $c = 7.729(2)$ Å, $\beta = 96.42(2)°$, using 51 reflections in the refinement. A few reflections were not indexed.

A sample of the intermediate phase of $Zn_3(AsO_4)_2$ was produced by a controlled heating to 500 °C using the DSC equipment. The powder pattern showed line broadening due to low crystal quality and/or the small size of the crystallites of the dehydrated material. Table 4 gives the observed *d* spacings of 37 reflections, with I/I_0 >5%, for this new polymorph of $Zn_3(AsO_4)_2$. The powder patterns of $Zn_9(AsO_4)_6{\cdot}4H_2O$ and those of the two phases found in the DSC experiment are compared in Fig. 3. A few reflections dominate the powder pattern of $Zn_9(AsO_4)_6{\cdot}4H_2O$ due to preferred orientation of the crystallites. This leads to the reaction scheme

$$Zn_9(AsO_4)_6{\cdot}4H_2O \xrightarrow{424\ ^\circ C} Zn_3(AsO_4)_2 \xrightarrow{865\ ^\circ C} \beta\text{-}Zn_3(AsO_4)_2.$$

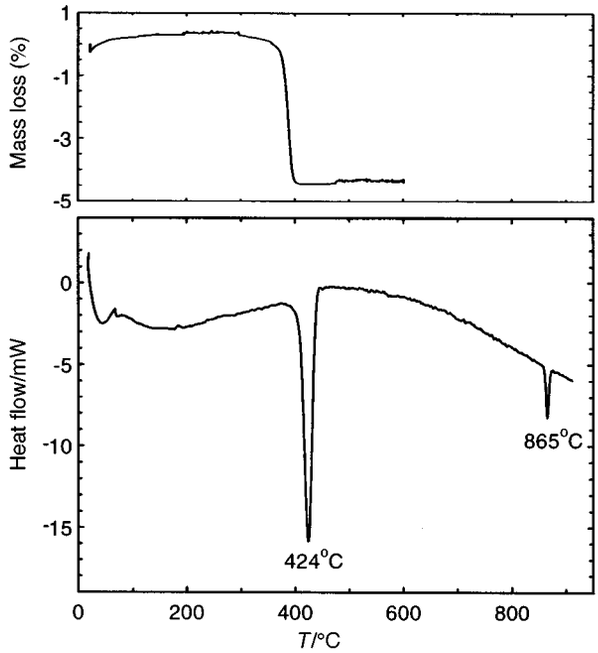

Fig. 2 Thermal investigation of $Zn_9(AsO_4)_6{\cdot}4H_2O$ showing the mass loss detected by thermogravimetry (upper curve) and differential scanning calorimetry

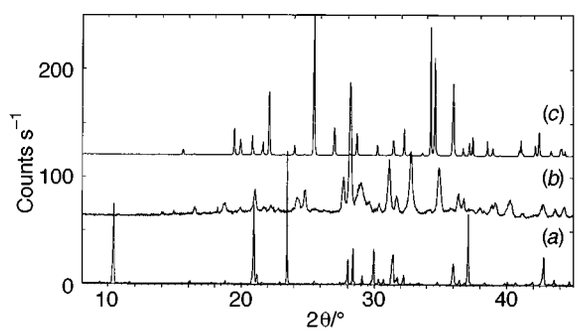

Fig. 3 Powder diffraction patterns of (*a*) $Zn_9(AsO_4)_6{\cdot}4H_2O$, (*b*) the material $Zn_3(AsO_4)_2$, formed at 500 °C and (*c*) β-$Zn_3(AsO_4)_2$

In the crystal structure of $Zn_9(AsO_4)_6{\cdot}4H_2O$ the water molecules are co-ordinated to the zinc ions forming octahedra [Zn(1), Zn(3) and Zn(4)]. The co-ordination flexibility of the zinc ions might allow a dehydration where the octahedra change to tetrahedra or trigonal bipyramids with minor changes in the framework structure. Structural similarities might exist between $Zn_9(AsO_4)_6{\cdot}4H_2O$ and the new phase of $Zn_3(AsO_4)_2$ formed at 424(1) °C.

Acknowledgements

Dr. O. Simonsen is thanked for valuable discussions and for the single-crystal measurements, using the CAD-4F instrument. The research carried out at the National Synchroton Light Source at Brookhaven National Laboratory is supported under contract DE-AC02-76CH00016 with the US Department of Energy by its Division of Chemical Science, Office of Basic Energy Science. The Danish Technical Research Council and the Danish Natural Science Research Council have supported this investigation with grants.

References

1 (*a*) R. J. Hill, *Am. Miner.*, 1979, **64**, 376; (*b*) J. M. Rojo, J. L. Mesa, J. L. Pizarro, L. Lezama, M. I. Arriortua and T. Rojo, *Mater. Res. Bull.*, 1996, **31**, 925.
2 A. Whitaker, *Acta Crystallogr.*, *Sect. B*, 1975, **31**, 2026; G. Y. Chao, *Z. Kristallogr.*, 1969, **130**, 261.

3 E. Sahakian and Y. Arnaud, *C. R. Acad. Sci.*, *Ser. 2*, 1988, **306**, 277.
4 A. Riou, Y. Cudennec and Y. Gerault, *Rev. Chim. Miner.*, 1986, **23**, 810.
5 C. Calvo, *Can. J. Chem.*, 1965, **43**, 436; J. S. Stephens and C. Calvo, *Can. J. Chem.*, 1967, **45**, 2303; C. Calvo, *J. Phys. Chem. Solids*, 1963, **24**, 141.
6 M. A. Nabar and V. S. Patkar, *Bull. Soc. Fr. Mineral. Cristallogr.*, 1974, **97**, 479.
7 H. Riffel, P. Keller and H. Hess, *Tschermaks Mineral. Petrogr. Mitt.*, 1980, **27**, 187; P. Keller, H. Hess and P. J. Dunn, *Neues Jahr. Miner. Monatsch.*, 1979, **9**, 389.
8 P. Keller, H. Riffel and H. Hess, *Z. Kristallogr.*, 1982, **158**, 33.
9 D. Frerichs, C. H. Park and Hk. Müller-Buschbaum, *Z. Naturforsch.*, *Teil B*, 1996, **51**, 333.
10 (*a*) R. J. Hill, *Am. Mineral.*, 1976, **61**, 979; (*b*) W. T. A. Harrison, J. T. Vaughey, L. L. Dussac, A. J. Jacobson, T. E. Martin and G. D. Stucky, *J. Solid State Chem.*, 1995, **114**, 151; (*c*) P. Keller, H. Hess and F. Zettler, *Neues Jahr. Miner. Monatsch.*, 1975, **134**, 147.
11 T. R. Jensen, P. Norby and J. C. Hanson, NSLS Activity Report 1996, BNL 52517, Brookhaven National Laboratory, Upton, NY, 1996, p. B-79; P. Feng, X. Bu and G. D. Stucky, *Acta Crystallogr.*, *Sect. C*, 1997, **53**, 997.
12 T. R. Jensen, P. Norby, J. C. Hanson, O. Simonsen, E. M. Skou, P. C. Stein and H. A. Boye, *J. Mater. Chem.*, in the press.
13 N. O. Ersson, CELLKANT, Chemical Institute, Uppsala University, Uppsala, 1981.
14 W. Kraus and G. Nolze, *J. Appl. Crystallogr.*, 1996, **29**, 301.
15 H. J. Jakobsen, P. Daugaard and V. Langer, *J. Magn. Reson.*, 1988, **76**, 162; *US Pat.*, 4 739 270, 1988.
16 N. F. Gmur, *NSLS users manual: Guide to the VUV and X-ray Beamlines*, Informal Report 48724, 5th edn., Brookhaven National Laboratory, Upton, NY, 1993; J. B. Hastings, P. Suortti, W. Thomlinson, A. Kvick and T. F. Koetzle, *Nucl. Instrum. Methods*, 1983, **208, 55.**
17 W. Minor, XDISPLAYF, Purdue University, 1993; Z. Otwinowski, Oscillation Data Reduction Program, compiled by L. Sawyer, in *Proceedings of the CCP4 study weekend: Data collection and Processing*, 29–30th January, 1993, p. 56.
18 A. J. C. Wilson, *International Tables for Crystallography*, Kluwer, Dordrecht, 1992, vol. C; D. R. Lide, *CRC Handbook of Chemistry and Physics*, CRC press, Boca Raton, FL, 74th edn., 1993.
19 D. T. Cromer, *J. Appl. Crystallogr.*, 1983, **16**, 437; A. C. Larson and R. B. Von Dreele, GSAS, General Structure Analysis System, Report LAUR 86-748, Los Alamos National Laboratory, NM, 1994.
20 G. M. Sheldrick, SHELXTL, Siemens Analytical X-ray Systems Inc., Madison, WI, 1995.
21 S. R. Hall, H. D. Flack and J. M. Stewart (Editors), *Xtal3.2 Reference Manual*, Universities of Western Australia and Maryland, 1992.
22 I. D. Brown and D. Altermatt, *Acta Crystallogr.*, *Sect. B*, 1985, **41**, 244.

Received 22*nd September* 1997; *Paper* 7/06827A